Supporting Information for

5-Fluorouracil Cocrystals with Lipophilic Hydroxy-2-Naphthoic Acids: Crystal Structures, Theoretical computations, and Permeation Studies

Xia-Lin Dai, Alexander P. Voronin, Yong-Liang Huang, German L. Perlovich, Xing-Hua Zhao, Tong-Bu Lu, Jia-Mei Chen*

Table of Contents

Experimental Section

Materials and Reagents. 5FU was purchased from Suizhou hongqi Chemical Co. Ltd. 6-Hydroxy-2-naphthoic acid (6HNA), 3-hydroxy-2-naphthoic acid (3HNA), and 1-hydroxy-2-naphthoic acid (1HNA) were purchased from Energy Chemical Co. Ltd. Isopropyl myristate (IPM) was purchased from Macklin Reagent Co. Ltd. All other reagents and chemicals were commercially available and used directly.

General Characterization Methods. Elemental analyses were determined using

Elementar Vario EL elemental analyzer. Powder X-ray diffraction (PXRD) patterns were recorded on a Bruker D2 Phaser with Cu Kα radiation (30 kV, 10 mA). Thermogravimetric (TG) analyses were recorded on a Netzsch TG 209 instrument and alumina crucible in nitrogen atmosphere from 37 °C to 500 °C at a heating rate of 10 °C/min. Differential scanning calorimetry (DSC) was conducted on a Netzsch DSC 200 F3 instrument and aluminum sample pans in nitrogen atmosphere from 37 °C at a heating rate of 10 °C/min. Infrared (IR) spectra were recorded on a Thermo Nicolet6700-Contiuμm spectrometer using KBr pellets. A total of 16 scans were collected over a range of 4000 to 400 cm^{-1} with a resolution of 0.09 cm^{-1} for each sample.

Screening of Cocrystals. In the present study, both neat grinding and liquid-assisted grinding were used to screen cocrystals of 5FU with xHNAs. A typical neat grinding experiment was conducted by adding an equimolar of 5FU (130 mg, 1 mmol) and xHNA (188 mg, 1 mmol) to a 25 mL stainless steel grinding jar. The mixture was then ground at a frequency of 20 Hz for 30 min. The liquid-assisted grinding procedure is similar to the neat grinding method, except adding 30 μL of solvent before grinding. A series of solvents with different polarity, including methanol, ethanol, acetone, acetonitrile, ethyl acetate, tetrahydrofuran, isopropyl ether, cyclohexane and dichloromethane, were attempted for 5FU with 1HNA, while only ethanol was sued for 5FU with 3HNA and 6HNA.

Preparation of Cocrystals. 5FU-3HNA was prepared by a slurry method. A mixture of 1 mmol 5FU (130 mg) and 0.5 mmol 3HNA (94 mg) was added to 1 mL

50% ethanol and stirred for 24 h. The resulting suspension was filtered and the filter cake was dried under vacuum at room temperature. Yield: 77%. Anal. (%) Calcd for $C_{19}H_{14}F_2N_4O_7$: C, 50.89; H, 3.15; N, 12.49. Found: C, 50.82; H, 3.24; N, 12.67. **5FU-6HNA** was obtained by a similar slurry procedure to that of **5FU-3HNA**, except using 1 mmol 6HNA (188 mg) instead of 0.5 mmol 3HNA. Yield: 78%. Anal. (%) Calcd for $C_{15}H_{11}FN_2O_5$: C, 56.60; H, 3.49; N, 8.80. Found: C, 56.02; H, 3.68; N, 8.84. Single crystals of both **5FU-3HNA** and **5FU-6HNA** were obtained from an evaporation process. A stoichiometric mixture of 5FU (130 mg, 1 mmol) and 3HNA (94 mg, 0.5 mmol) or 6HNA (188 mg, 1 mmol) was added to 4 mL 50% ethanol and was then treated under ultrasonic irradiation for 20 min. The resulting suspension was filtered and the filtrate was left to slowly evaporate at room temperature. Block-shaped crystals of **5FU-3HNA** and **5FU-6HNA** were harvested after 2−3 days.

X-ray Crystal Structure Determination. Single crystal X-ray diffraction data were collected on an Agilent Technologies Gemini A Ultra system with graphite monochromated Cu Kα radiation (λ = 1.54178 Å) at 150 K. Cell refinement and data reduction were applied using the program of CrysAlis PRO.[1] The structures were solved by the direct method using the SHELX-97 program[2] and refined by the full-matrix least-squares method on F^2. All non-hydrogen atoms were refined with anisotropic displacement parameters. All hydrogen atoms were placed in calculated positions with fixed isotropic thermal parameters. For crystal structure of **5FU-3HNA**, two crystallographically independent 3HNA molecules were found to be disordered over two positions with occupancy ratio of 0.75/0.25 and 0.50/0.50, respectively.

Membrane Permeation Experiments. The permeation experiments of pure 5FU, 6HNA, 3HNA, the two cocrystals and their respective stoichiometric physical mixtures were conducted using Franz-type diffusion cells through silicon membrane (120 μm thickness). All of the powder samples were sieved using standard mesh sieves to control the particle size within 75−150 μm. The silicon membrane was pretreated with 95% ethanol for 30 min and dried under air before use. The silicon membrane was mounted between donor chamber and receptor chamber with an effective surface area of 3.14 cm^2. The receptor chamber was filled with 17 mL of degassed phosphate buffer (pH 7.4) and maintained at 37.0 ± 0.1 °C, and the receptor solution was stirred at 250 rpm for 30 min to reach system balance. Excess of powder samples (0.3 mmol) were added to 1 mL of IPM and mixed well. The resulting suspensions were placed on the silicon membrane as donor chamber. An aliquot of 0.2 mL of the receptor solution was withdrawn from the receptor chamber and filtered at predetermined time intervals. The receptor chamber solution volume was kept constant by replacing fresh medium. During the experiment, the receptor solution maintained at 37.0 ± 0.1 °C and was continuously stirred at 250 rpm. The concentration of 5FU for each sample was analyzed by HPLC. After the permeation experiments, the remaining solids in donor chamber were collected and detected by PXRD to check the crystalline phase. All the permeation experiments were repeated three times (n = 3).

Solubility Study. The aqueous solubility of 5FU, 6HNA, 3HNA and two cocrystals in pH 6.8 phosphate buffer solution (PBS) were determined. All of the powder

samples were sieved using standard mesh sieves to control the particle size within 75−150 μm. In each experiment, excess of sample (200−500 mg) was added to 5 mL of 0.2 M pH 6.8 PBS which was equilibrated at 37 ºC, and the resulting slurry was stirred at 250 rpm on a magnetic stirrer. Aliquots were filtered after 1 h, 3 h and 5 h, respectively. Each filtered aliquot was diluted to the approximate concentration and was analyzed by HPLC. After the solubility determination, the remaining solids were collected and detected by PXRD. All the experiments were carried out in triplicate (n = 3).

Powder dissolution experiments in IPM were also carried out for 5FU and two cocrystals. Excess of 5FU and its cocrystals (contains 100 mg of 5FU) with particle size within 75−150 μm were suspended in 5 mL of IPM, which were preheated at 37 °C for 30 min. The suspensions were kept magnetic stirring at 150 rpm and 37 °C. An aliquot of the slurry was withdrawn at predetermined time intervals and filtered. The filtered aliquot was appropriately diluted and measured by HPLC to quantify 5FU concentrations. After the dissolution, the remaining solids were collected and detected by PXRD. The experiments were carried out in triplicate (n = 3).

HPLC Analysis Method. HPLC analysis was performed on A Shimadzu LC-20A HPLC system with a C18 column (Inertsil ODS-3, 5 μm × 4.6 mm × 150 mm column, GL Sciences Inc., Japan). UV detection wavelength of 266 nm was used for assay of 5FU and 3HNA while 237 nm for 6HNA. The mobile phase consisted of a mixture of methanol and aqueous phosphoric acid solutions (pH 2.40). The gradient elution was used with a flow rate of 0.7 mL/min. It was started with 10% (v/v) methanol (6 min),

followed by an increase to 90% (v/v) methanol (7 min), reserved at 90% (v/v) methanol (23 min), and returned immediately to 10% (v/v) methanol (23.5 min), and then reserved at 10% (v/v) methanol (30 min).

Computational Details. Solid-state DFT computations were performed using CRYSTAL17 software[3] at the B3LYP-D3/6-31(F+)G(d, p) level of theory. D3 dispersion correction proposed by Grimme[4] with Becke-Jones dampening was used both in structure optimization and in wave function calculation for AIM analysis. For a more adequate description of fluorine-centered contacts in 5FU crystals, an additional polarization function was added to the fluorine atoms.[5] The space groups and unit cell parameters of the both cocrystals obtained in the single crystal X-ray studies were fixed and structural relaxations were limited to the positional parameters of atoms. As the starting point in the solid-state DFT computations, the coordinates of heavy atoms were used directly from experiment with hydrogen atoms positions normalized to the standard X–H distances from neutron diffraction data. The default CRYSTAL options were used for the level of accuracy in evaluating the Coulomb and Hartree-Fock exchange series and a grid used in evaluating the DFT exchange-correlation contribution. Tolerance on energy controlling the self-consistent field convergence for geometry optimizations and frequencies computations was set to 10^{-10} hartree. The mixing coefficient of Hartree-Fock/Kohn-Sham matrices was set to 25%. The number of points in the numerical first derivative calculation of the analytic nuclear gradients equaled 2. The shrinking factor of the reciprocal space net was set to 3. Frequencies of normal modes were calculated within the harmonic approximation by numerical

differentiation of the analytical gradient of the potential energy with respect to atomic position.[6] Based on vibrational analysis, all the optimized structures were found to correspond to the minimum point on the potential energy surface.

Quantum topology analysis was performed in Topond software[7] currently implemented into CRYSTAL suit. The search for (3, −1) critical points was performed using a standard algorithm and the following quantities were computed in bond critical point (BCP): electron density, ρ_b, its Laplacian, $\nabla^2\rho_b$, and the positively defined local electronic kinetic energy G_b. The energy of a particular noncovalent interaction, E_{int}, was estimated using the correlation equation proposed by Mata *et al*:[8]

$$E_{int}\ (\text{kJ/mol}) = 1124 \cdot G_b\ (\text{atomic units}) \qquad \text{(S1)}$$

The lattice energy E_{latt} was estimated as sum of energies of unique intermolecular interactions in an asymmetric unit:[9]

$$\text{E}_{\text{latt}}\ (\text{kJ/mol}) = \sum_i \sum_{j<i} E_{\text{int},j,i} \qquad \text{(S2)}$$

where j and i denote the atoms belonging to different molecules. Eq. (S2) is free of basis set superposition error (BSSE). For the sake of simplicity, indices j and i will be omitted below.

For a cocrystal (CC) of composition [API-CCF] (x:y), the formation energy can be estimated from the lattice energies according to the following equation:

$$E_{form} = \text{x}\ E_{\text{latt}}(\text{API}) + \text{y}\ E_{\text{latt}}(\text{CCF}) - E_{\text{latt}}(\text{CC}) \qquad \text{(S3)}$$

An alternative way for E_{form} estimation implies the use of the raw total energies and thermodynamic quantities of crystals obtained from periodic DFT-D3 calculations. In this case, the equation for formation energy has the following form:

$$E_{form} = E_{\text{total}}(\text{CC}) - \text{x}\ E_{\text{total}}(\text{API}) - \text{y}\ E_{\text{total}}(\text{CCF}) \quad \text{(S4)}$$

The estimations of heat capacity and entropy at 298.15 K in periodic DFT computations, although crude, allow one to compute the total Gibbs energy of crystal (G_{total}) and free Gibbs energy of the cocrystal formation reaction (G_{form}):

$$G_{\text{total}} = E_{\text{total}} + \text{ZPE} + E_{\text{therm}} + \text{pV} - \text{TS} \quad \text{(S5)}$$

$$G_{form} = G_{\text{total}}(\text{CC}) - \text{x}\ G_{\text{total}}(\text{API}) - \text{y}\ G_{\text{total}}(\text{CCF}) \quad \text{(S6)}$$

Since the vibration analysis was performed in a harmonic approximation, the values of heat capacities and entropy contributions obtained this way are less reliable than total energies at conventional zero Kelvin. For this reason, we present the values of both formation energies (E_{form}) and formation free Gibbs energies (G_{form}) in the manuscript. While the latter quantity is more physically meaningful, the former is more reliable.

REFERENCES

(1) *CrysAlisPro*; Agilent Technologies Inc.: Santa Clara, CA.

(2) Sheldrick, G. M. *SHELXTL-97, Program for Crystal Structure Solution and Refinement.* University of Göttingen: Göttingen, Germany, **1997**.

(3) Dovesi, R.; Erba, A.; Orlando, R.; Zicovich-Wilson, C. M.; Civalerri, B.; Maschio, L.; Rerat, M.; Casassa, S.; Baima, J.; Salustro, S.; Kirtman, B. "Quantum-mechanical using CRYSTAL17. WIREs" *Comput. Mol. Sci.* **2018**, *8*, e1360.

(4) Grimme, S.; Antony, J.; Ehrlich, S.; Krieg, H. "A consistent and accurate ab initio parametrization of density functional dispersion correction (DFT-D) for the 94 elements H-Pu" *J. Chem. Phys.* **2010**, *132*, 154104

(5) Levina, E. O.; Chernyshov, I. Y.; Voronin, A. P.; Alekseiko, L. N.; Stash, A. I.; Vener, M. V. "Solving the enigma of weak fluorine contacts in the solid state: a periodic DFT study of fluorinated organic crystals" *RSC Adv.* **2019,** *9*, 12520–12537.

(6) Pascale, F.; Zicovich-Wilson, C. M.; Gejo, F. L.; Civalleri, B.; Orlando, R.; Dovesi, R. "The calculation of vibrational frequencies of crystalline compounds and its implementation in the CRYSTAL code" *J. Comput. Chem.* **2004**, *25*, 888–897.

(7) Gatti, C.; Saunders, V. R.; Roetti, C. "Crystal field effects on the topological properties of the electron density in molecular crystals. The case of urea" *J. Chem. Phys.* **1994**, *101*, 10686–10696.

(8) Mata, I.; Alkorta, I.; Espinosa, E.; Molins, E. "Relationships between interaction energy, intermolecular distance and electron density properties in

hydrogen bonded complexes under external electric fields" *Chem. Phys. Lett.* **2011**, *507*, 185–189.

(9) Dominiak, P. M.; Espinosa, E.; Angyan, J. *in Modern charge density analysis*, ed. Gatti, C. and Macchi, P. Springer, Heidelberg, London, New York, **2012**, pp. 387–433.

Table S1. Hydrogen Bonding Distances and Angles of 5FU-6HNA and 5FU-3HNA

hydrogen bond	H···A (Å)	D···A (Å)	∠D–H···A (°)	symmetry
5FU-6HNA				
N3−H3···O2	1.931	2.787(18)	173.58	-x-1/2, y+1/2, -z+3/2
N5−H5···O2	2.033	2.845(18)	157.10	-x-1/2, y-1/2, -z+3/2
O7−H7···O4	1.963	2.705(17)	150.15	
O10−H10···O16	1.814	2.633(17)	176.38	-x+2, -y+1, -z+2
5FU-3HNA				
O9−H9···O10	1.86	2.600(3)	145.4	
O11−H11···O8	1.87	2.711(3)	177.5	
O12−H12···O13	1.87	2.603(6)	144.9	
O14−H14···O6	1.88	2.710(4)	170.5	
O9A−H9A···O10A	1.91	2.625(15)	142.7	
O11A−H11A···O4	2.10	2.740(8)	133.3	+x, -1+y, -1+z
O12A−H12A···O13A	1.87	2.609(5)	145.7	
O14A−H14A···O2	1.88	2.712(4)	169.3	
N1−H1A···O7	1.92	2.795(3)	175.4	1-x, 1-y, 1-z
N6−H6···O3	1.90	2.778(3)	173.1	

Table S2. Metric and Electron Density Properties in Bond Critical Point of Noncovalent Interactions in 5FU-6HNA Obtained from Periodic DFT Calculations Followed by Bader Analysis of Periodic Electron Density *

non-covalent interaction	D···A (Å) | H···A (Å)	∠D–H···A (°)	ρ_b (a.u.)	$\nabla^2\rho_b$ (a.u.)	G_b (a.u.)	E_{int} (kJ/mol)
O10–10···O16[a]	2.605 | 1.595	177.49	0.057	0.155	0.043	**48.2**
O7–H7···O4[b]	2.662 | 1.750	152.69	0.037	0.124	0.029	**33.2**
N3–H3···O2[c]	2.788 | 1.757	174.49	0.039	0.117	0.029	**32.6**
N5–H5···O2[d]	2.821 | 1.815	164.98	0.034	0.101	0.025	**28.4**
C22–H22···F1[b]	3.236 | 2.267	147.90	0.011	0.044	0.010	**11.5**
C9–H9···O4[e]	3.436 | 2.462	149.20	0.008	0.030	0.007	**7.5**
C20–H20···F1[f]	3.105 | 2.656	104.20	0.006	0.030	0.006	**6.6**
N3···O10[g]	3.114	-	0.008	0.024	0.006	**6.5**
C9–H9···O7[e]	3.395 | 2.541	135.19	0.007	0.026	0.006	**6.3**
C17···O16[f]	3.126	-	0.007	0.024	0.005	**5.7**
H21···H13[e]	2.189	-	0.007	0.025	0.005	**5.4**
C22–H22···O7[h]	3.395 | 2.735	119.01	0.006	0.023	0.005	**5.4**
C13···C9[c]	3.218	-	0.008	0.021	0.004	**4.8**
O7···F1[i]	3.198	-	0.004	0.021	0.004	**4.7**
C18···O2[j]	3.298	-	0.006	0.020	0.004	**4.7**
C11···N5[j]	3.386	-	0.006	0.017	0.004	**4.2**
C21···N3[j]	3.455	-	0.005	0.016	0.003	**3.8**
H12···H21[k]	2.534	-	0.005	0.018	0.003	**3.8**
C14···C6[j]	3.370	-	0.005	0.017	0.003	**3.7**
N5···O16[l]	3.399	-	0.004	0.015	0.003	**3.6**
O7···O10[f]	3.412	-	0.003	0.015	0.003	**3.5**
C19···C11[f]	3.477	-	0.005	0.013	0.003	**3.0**
C14···C13[f]	3.533	-	0.004	0.013	0.003	**2.9**
C11–H11···O2[m]	3.781 | 3.036	126.37	0.003	0.012	0.002	**2.6**
H11···H21[e]	2.599	-	0.003	0.011	0.002	**2.3**
H13···H12[e]	2.662	-	0.003	0.010	0.002	**2.0**
E_{latt} (kJ/mol)						**246.9**

* The electron density ρ_b, Laplacian of electron density $\nabla^2\rho_b$ and local electronic kinetic energy density G_b at the bond critical point; the energy of the intermolecular noncovalent interaction E_{int}. The level of theory in the DFT computations is B3LYP-D3(BJ)/6-31(F+)G(d,p).

Symmetry codes: [a] 2-x, 1-y, -z; [b] x, y, z; [c] -1/2-x, 1/2+y, -1/2-z; [d] -1/2-x, -1/2+y, -1/2-z; [e] x, -1+y, z; [f] 1-x, 1-y, -z; [g] -1+x, y, z; [h] 1/2-x, -1/2+y, -1/2-z; [i] x,1+y, z; [j] 1/2-x, 1/2+y, -1/2-z; [k] 1-x, 2-y, -z; [l] -1+x, -1+y, z; [m] 1+x, y, z

Table S3. Metric and Electron Density Properties in Bond Critical Point of Noncovalent Interactions in 5FU-3HNA (Conformation 1) Obtained from Periodic DFT Calculations Followed by Bader Analysis of Periodic Electron Density *

non-covalent interaction	D···A (Å) | H···A (Å)	∠D–H···A (°)	ρ_b (a.u.)	$\nabla^2\rho_b$ (a.u.)	G_b (a.u.)	E_{int} (kJ/mol)
O12–H12···O13[a]	2.587 | 1.697	147.89	0.048	0.140	0.037	**41.4****
O9–H9···O10[a]	2.591 | 1.703	147.27	0.047	0.138	0.036	**40.9****
O14–H14···O6[b]	2.665 | 1.663	178.31	0.048	0.137	0.035	**39.6**
O11–H11···O8[c]	2.677 | 1.674	176.64	0.046	0.132	0.034	**37.8**
N6–H6···O3[d]	2.748 | 1.715	176.39	0.043	0.131	0.032	**36.4**
N8–H8···O5[e]	2.759 | 1.727	175.62	0.042	0.125	0.031	**35.3**
N1–H1A···O7[f]	2.767 | 1.732	177.15	0.041	0.124	0.031	**34.8**
N3–H3···O5[a]	2.781 | 1.749	178.71	0.039	0.120	0.030	**33.4**
N2–H2···O3[g]	2.862 | 1.838	172.73	0.032	0.094	0.023	**26.4**
N7–H7···O1[h]	2.872 | 1.853	170.00	0.031	0.090	0.022	**25.3**
N4–H4···O1[a]	2.897 | 1.880	167.52	0.029	0.082	0.021	**23.6**
N5–H5···O7[i]	2.955 | 1.939	170.10	0.026	0.071	0.018	**20.7**
C13–H13···O4[e]	3.170 | 2.113	163.97	0.018	0.055	0.014	**15.3**
C25–H25···F4[e]	3.030 | 2.182	133.40	0.013	0.055	0.013	**14.2**
C36–H36···F3[j]	3.070 | 2.231	132.76	0.013	0.050	0.012	**13.2**
C9–H9A···O2[e]	3.243 | 2.227	155.07	0.014	0.044	0.011	**12.0**
C5–H5A···O10[k]	3.131 | 2.285	133.51	0.013	0.043	0.010	**11.5**
O14···F3[b]	2.787	-	0.009	0.045	0.010	**10.9**
H26···H26[l]	1.961	-	0.012	0.043	0.009	**10.3**
O13···F1[m]	2.840	-	0.009	0.038	0.009	**9.7**
O11···F4[c]	2.845	-	0.008	0.039	0.008	**9.4**
C1–H1···O13[m]	3.218 | 2.414	129.84	0.010	0.035	0.008	**8.8**
C17–H17···O9[k]	3.447 | 2.418	157.95	0.010	0.033	0.008	**8.8**
O10···F2[k]	2.900	-	0.008	0.035	0.008	**8.6**
C13···F3[a]	2.931	-	0.008	0.034	0.007	**8.1**
C28–H28···O12[n]	3.498 | 2.507	151.67	0.009	0.029	0.007	**7.5**
H28···H28[n]	2.149	-	0.008	0.031	0.006	**6.7**
O9···O1[k]	3.176	-	0.006	0.025	0.006	**6.3**
O10···N7[k]	3.165	-	0.007	0.025	0.006	**6.3**
O14···N1[b]	3.184	-	0.007	0.024	0.005	**6.1**
C8···O2[a]	3.101	-	0.007	0.025	0.005	**6.0**
C18···O1[k]	3.166	-	0.006	0.025	0.005	**5.9**
H37···H37[o]	2.185	-	0.007	0.026	0.005	**5.7**
C5···F1[a]	3.143	-	0.005	0.025	0.005	**5.5**
C13···O12[a]	3.219	-	0.006	0.024	0.005	**5.5**
C9–H9A···O4[e]	3.269 | 2.749		0.006	0.023	0.005	**5.1**
O6···F4[a]	3.251	-	0.005	0.024	0.005	**5.1**
C35···O11[j]	3.215	-	0.006	0.021	0.004	**4.9**
C36–H36···O10[j]	3.324 | 2.834	107.55	0.006	0.021	0.004	**4.7**

C26···O5[e]	3.307	-	0.006	0.020	0.004	**4.7**
C31···O7[b]	3.259	-	0.006	0.020	0.004	**4.6**
C29···O4[e]	3.246	-	0.006	0.020	0.004	**4.6**
C16···O6[a]	3.258	-	0.005	0.019	0.004	**4.5**
C15···C33[n]	3.251	-	0.006	0.021	0.004	**4.5**
C34···O3[d]	3.291	-	0.006	0.019	0.004	**4.5**
C22···N8[a]	3.336	-	0.006	0.018	0.004	**4.5**
C26−H26···N3[e]	3.516 | 2.828	121.46	0.006	0.019	0.004	**4.5**
C1−H1···O6[h]	3.670 | 2.684	151.12	0.005	0.019	0.004	**4.4**
C24···N8[e]	3.319	-	0.006	0.017	0.004	**4.3**
C23···O13[e]	3.312	-	0.005	0.018	0.004	**4.3**
C21···N7[c]	3.407	-	0.006	0.017	0.004	**4.2**
H17···H17[k]	2.370	-	0.005	0.020	0.004	**4.1**
C37···O8[o]	3.404	-	0.005	0.017	0.004	**4.0**
C5···C2[a]	3.310	-	0.005	0.018	0.004	**4.0**
C32···N2[e]	3.414	-	0.006	0.016	0.004	**4.0**
O14···F2[e]	3.285	-	0.003	0.018	0.004	**4.0**
C28···N1[n]	3.497	-	0.005	0.016	0.004	**4.0**
C35−H35···O2[d]	3.798 | 2.780	155.94	0.005	0.017	0.003	**3.8**
C1···C22[p]	3.393	-	0.005	0.017	0.003	**3.8**
C23···O5[a]	3.368	-	0.005	0.016	0.003	**3.7**
C24−H24···O4[a]	3.759 | 2.799	147.39	0.004	0.016	0.003	**3.7**
C37−H37···C5[q]	3.534 | 2.925	115.70	0.005	0.017	0.003	**3.7**
H20···H26[l]	2.445	-	0.005	0.017	0.003	**3.6**
C23−H23···F2[a]	3.726 | 2.740	150.88	0.004	0.017	0.003	**3.6**
H31···H37[o]	2.417	-	0.005	0.016	0.003	**3.4**
C35···N2[d]	3.482	-	0.005	0.014	0.003	**3.4**
C20−H20···O2[e]	3.493 | 2.986	108.98	0.004	0.015	0.003	**3.2**
C28−H28···N6[a]	3.651 | 2.992	119.69	0.004	0.014	0.003	**3.2**
C34−H34···O12[n]	3.801 | 2.909	139.58	0.004	0.014	0.003	**3.0**
C5−H5A···O8[h]	3.800 | 2.859	145.26	0.003	0.014	0.003	**3.0**
C19···C9[a]	3.532	-	0.005	0.013	0.003	**3.0**
C2···C25[p]	3.530	-	0.005	0.013	0.003	**2.9**
C36···O3[e]	3.584	-	0.003	0.012	0.002	**2.8**
***E*$_{latt}$ (kJ/mol)**						**333.5**

[*] The electron density ρ_b, Laplacian of electron density $\nabla^2\rho_b$ and local electronic kinetic energy density G_b at the bond critical point; the energy of the intermolecular noncovalent interaction E_{int}. The level of theory in the DFT computations is B3LYP-D3(BJ)/6-31(F+)G(d,p).

[**] Intramolecular contact. The energy of this interaction does not count in the total E_{latt} value.

Symmetry codes: [a] x,y,z; [b] -1+x,y,z; [c] x,1+y,z; [d] x,y,1+z; [e] -x,-y,-z; [f] 1-x,-1-y,1-z; [g] -x,-y,-1-z; [h] 1-x,-1-y,-z; [i] x,y,-1+z; [j] -x,-y,1-z; [k] 1-x,-y,-z; [l] -x,1-y,-z; [m] -x,-1-y,-z; [n] -x,-1-y,1-z; [o] -1-x,-y,1-z; [p] x,-1+y,z; [q] -1+x,y,1+z.

Table S4. Metric and Electron Density Properties in Bond Critical Point of Noncovalent Interactions in 5FU-3HNA (Conformation 2) Obtained from Periodic DFT Calculations Followed by Bader Analysis of Periodic Electron Density *

non-covalent interaction	D···A (Å) | H···A (Å)	∠D–H···A (°)	ρ_b (a.u.)	$\nabla^2\rho_b$ (a.u.)	G_b (a.u.)	E_{int} (kJ/mol)
O9–H9···O10[a]	2.592 | 1.709	146.66	0.047	0.137	0.036	**40.3****
O14–H14···O2[a]	2.663 | 1.662	176.67	0.048	0.138	0.035	**39.8**
O12–H12···O13[a]	2.600 | 1.712	147.24	0.046	0.135	0.035	**39.6****
O11–H11···O8[b]	2.670 | 1.667	178.39	0.047	0.135	0.035	**39.0**
N6–H6···O3[c]	2.730 | 1.695	176.58	0.045	0.137	0.034	**38.5**
N7–H7···O1[d]	2.737 | 1.704	175.21	0.044	0.133	0.033	**37.5**
N1–H1A···O7[e]	2.773 | 1.738	176.31	0.041	0.122	0.030	**34.0**
N4–H4···O1[a]	2.777 | 1.752	172.82	0.039	0.121	0.030	**33.5**
N2–H2···O3[f]	2.850 | 1.824	173.91	0.033	0.098	0.024	**27.5**
N3–H3···O5[a]	2.876 | 1.846	173.03	0.032	0.089	0.023	**25.4**
N8–H8···O5[g]	2.899 | 1.877	172.20	0.029	0.084	0.021	**23.8**
N5–H5···O7[h]	2.951 | 1.937	169.26	0.026	0.072	0.018	**20.8**
C13–H13···O4[g]	3.149 | 2.078	168.13	0.019	0.058	0.015	**16.4**
C25–H25···F4[g]	3.050 | 2.147	139.41	0.014	0.057	0.013	**15.1**
C36–H36···F1[i]	3.035 | 2.220	130.35	0.013	0.052	0.012	**13.6**
C1–H1···O6[d]	3.226 | 2.200	156.87	0.015	0.047	0.011	**12.6**
C5–H5A···O10[j]	3.118 | 2.254	135.22	0.014	0.045	0.011	**12.1**
F1···O14[a]	2.776	-	0.009	0.045	0.010	**11.0**
F3···O13[g]	2.812	-	0.009	0.040	0.009	**10.2**
H26···H26[k]	1.935	-	0.012	0.040	0.009	**10.0**
O11···F4[b]	2.838	-	0.008	0.041	0.009	**9.7**
C28–H28···O12[l]	3.457 | 2.443	155.30	0.010	0.032	0.007	**8.4**
O10···F2[i]	2.928	-	0.007	0.034	0.007	**8.3**
O9–H9···F2[i]	3.086 | 2.422	124.00	0.007	0.035	0.007	**8.1**
C9–H9A···O13[g]	3.683 | 2.694	151.49	0.009	0.032	0.007	**8.0**
C13···F3[a]	2.958	-	0.008	0.033	0.007	**7.8**
H37···H37[i]	2.082	-	0.009	0.032	0.007	**7.4**
C17–H17···O9[j]	3.510 | 2.512	152.75	0.009	0.029	0.007	**7.3**
O11···O13[g]	3.129	-	0.007	0.025	0.006	**6.4**
O10···N7[j]	3.203	-	0.007	0.025	0.005	**6.1**
N2···O14[a]	3.208	-	0.007	0.023	0.005	**5.9**
C8···O2[a]	3.123	-	0.007	0.024	0.005	**5.9**
C5···F1[a]	3.101	-	0.006	0.026	0.005	**5.9**
H17···H17[j]	2.205	-	0.007	0.027	0.005	**5.8**
O6···F4[a]	3.209	-	0.005	0.026	0.005	**5.7**
H28···H28[l]	2.242	-	0.007	0.026	0.005	**5.4**
C5–H5A···O12[l]	3.263 | 2.777	107.00	0.006	0.024	0.005	**5.3**
C18···O1[j]	3.205	-	0.006	0.023	0.005	**5.3**
C26···O5[g]	3.327	-	0.006	0.021	0.004	**5.0**

C30···O8[n]	3.286	-	0.006	0.020	0.004	**4.8**
C16···O6[a]	3.229	-	0.006	0.020	0.004	**4.8**
C37−H37···C13[h]	3.378 | 2.825	111.58	0.006	0.021	0.004	**4.5**
C21···N7[b]	3.379	-	0.006	0.018	0.004	**4.4**
C9−H9A···O2[g]	3.683 | 2.694	151.49	0.005	0.019	0.004	**4.3**
C24−H24···O4[a]	3.730 | 2.730	153.06	0.005	0.019	0.004	**4.3**
C33···N2[f]	3.429	-	0.006	0.018	0.004	**4.3**
C9−H9A···O4[g]	3.324 | 2.831	107.64	0.005	0.020	0.004	**4.3**
C22···N8[a]	3.380	-	0.006	0.017	0.004	**4.2**
C37···O4[f]	3.380	-	0.005	0.017	0.004	**4.1**
C31···O3[a]	3.334	-	0.005	0.017	0.004	**4.0**
H20···H26[n]	2.372	-	0.005	0.019	0.003	**3.9**
C34···O7[o]	3.393	-	0.005	0.017	0.003	**3.9**
C28···C6[f]	3.430	-	0.005	0.018	0.003	**3.9**
C28···O7[o]	3.408	-	0.004	0.016	0.003	**3.8**
C32···N1[n]	3.441	-	0.005	0.015	0.003	**3.7**
H31···H37[i]	2.407	-	0.005	0.017	0.003	**3.7**
C23−H23···F2[a]	3.685 | 2.737		0.004	0.017	0.003	**3.6**
C19···C9[a]	3.414	-	0.006	0.016	0.003	**3.6**
C24···N8[g]	3.417	-	0.005	0.015	0.003	**3.6**
C24−H24···C36[f]	3.632 | 2.937	122.09	0.005	0.017	0.003	**3.5**
C34···C8[f]	3.404	-	0.005	0.016	0.003	**3.5**
O10···O12[g]	3.415	-	0.003	0.015	0.003	**3.4**
C35−H35···O6[o]	3.835 | 2.842	152.08	0.004	0.015	0.003	**3.3**
C34···N1[o]	3.492	-	0.005	0.014	0.003	**3.3**
C26−H26···N3[g]	3.678 | 2.984	122.25	0.004	0.014	0.003	**3.2**
C17−H17···O6[j]	3.508 | 3.065	105.20	0.004	0.014	0.003	**3.2**
C1−H1···O8[d]	3.520 | 2.964	112.15	0.003	0.015	0.003	**3.1**
C2···C26[p]	3.609	-	0.005	0.013	0.003	**3.0**
C23···O5[a]	3.499	-	0.003	0.013	0.003	**2.9**
C20−H20···O2[g]	3.605 | 3.016	114.61	0.003	0.013	0.003	**2.8**
C5−H5A···O8[d]	3.828 | 2.894	144.58	0.003	0.013	0.002	**2.8**
C17−H17···N4[j]	3.666 | 3.122	111.94	0.004	0.012	0.002	**2.8**
C23−H23···O9[j]	3.851 | 2.966	138.90	0.003	0.012	0.002	**2.7**
C35−H35···C23[f]	3.839 | 3.159	121.30	0.003	0.011	0.002	**2.3**
***E*$_{latt}$ (kJ/mol)**						**338.0**

[*] The electron density ρ_b, Laplacian of electron density $\nabla^2\rho_b$ and local electronic kinetic energy density G_b at the bond critical point; the energy of the intermolecular noncovalent interaction E_{int}. The level of theory in the DFT computations is B3LYP-D3(BJ)/6-31(F+)G(d,p).

[**] Intramolecular contact. The energy of this interaction does not count in the total E_{latt} value.

Symmetry codes: [a] x,y,z; [b] x,1+y,z; [c] x,y,1+z; [d] 1-x,-1-y,-z; [e] 1-x,-1-y,1-z; [f] -x,-y,-1-z; [g] -x,-y,-z; [h] x,y,-1+z; [i] -x,-1-y,-1-z; [j] 1-x,-y,-z; [k] -x,1-y,-z; [l] -1-x,-y,-1-z; [m] 1+x,y,z; [n] -x,-1-y,-z; [o] -1+x,y,-1+z; [p] x,-1+y,z.

Table S5. Contributions of Different Noncovalent Interaction Types into the Lattice Energy of 5FU-3HNA and 5FU-6HNA*

Crystal	**5FU-3HNA** (conformation 1)	**5FU-3HNA** (conformation 2)	**5FU-3HNA** (averaged)	**5FU-6HNA**
E_{latt}	**333.5**	**338.0**	**335.7**	**246.9**
5FU−5FU	154.5 (46.3%)	157.3 (46.5%)	155.9 (46.4%)	68.5 (27.7%)
5FU−HNA	145.4 (43.6%)	145.6 (43.1%)	145.5 (43.3%)	102.0 (41.3%)
HNA−HNA	33.5 (10.1%)	35.1 (10.4%)	34.3 (10.2%)	76.5 (31.0%)
Classical H-bonds	156.7 (47.0%)	164.0 (48.5%)	160.3 (47.8%)	142.4 (57.7%)
C−H···O contacts	47.4 (14.2%)	50.6 (15.0%)	49.0 (14.6%)	21.8 (8.8%)
C−H···N contacts	3.8 (1.2%)	3.0 (0.9%)	3.4 (1.0%)	0 (0%)
C−H···F contacts	15.5 (4.6%)	16.2 (4.8%)	15.8 (4.7%)	18.1 (7.3%)
C−H···π contacts	1.9 (0.6%)	5.2 (1.5%)	3.5 (1.0%)	0 (0%)
X···F contacts	30.7 (9.2%)	29.2 (8.6%)	29.9 (8.9%)	4.7 (1.9%)
π-stacking	60.6 (18.2%)	51.8 (15.3%)	56.2 (16.7%)	46.3 (18.8%)
H···H contacts	16.9 (5.1%)	18.1 (5.4%)	17.5 (5.2%)	13.5 (5.5%)
Intralayer contacts	249.3 (74.8%)	259.0 (76.6%)	254.1 (75.7%)	182.2 (73.8%)
Interlayer contacts	84.2 (25.2%)	79.0 (23.4%)	81.6 (24.3%)	64.7 (26.2%)

*All values are given in kJ/mol and % of the E_{latt} value.

Table S6. Metric and Electron Density Properties in Bond Critical Point of Noncovalent Interactions in 5FU (refcode FURACL14) Obtained from Periodic DFT Calculations Followed by Bader Analysis of Periodic Electron Density *

non-covalent interaction	D···A (Å) | H···A (Å)	∠D–H···A (°)	ρ_b (a.u.)	$\nabla^2\rho_b$ (a.u.)	G_b (a.u.)	E_{int} (kJ/mol)
N6–H8···O8[a]	2.796 | 1.761	175.60	0.039	0.114	0.028	**32.0**
N5–H7···O1[b]	2.798 | 1.768	171.83	0.035	0.115	0.027	**30.7**
N4–H5···O2[c]	2.817 | 1.785	174.57	0.037	0.108	0.027	**30.1**
N2–H2···O4[d]	2.819 | 1.790	174.39	0.036	0.107	0.027	**30.0**
N8–H11···O6[a]	2.823 | 1.797	172.77	0.036	0.106	0.026	**29.6**
N3–H4···O5[e]	2.847 | 1.820	175.07	0.031	0.100	0.024	**26.9**
N1–H1···O7[f]	2.850 | 1.830	171.02	0.030	0.098	0.023	**26.3**
N7–H10···O3[g]	2.861 | 1.843	170.20	0.030	0.094	0.023	**25.5**
C11–H9···O4[h]	3.103 | 2.062	159.46	0.021	0.060	0.016	**17.6**
C2–H3···O6[h]	3.132 | 2.088	160.55	0.020	0.057	0.015	**16.7**
C6–H6···O8[i]	3.126 | 2.109	154.77	0.020	0.055	0.014	**16.1**
C14–H12···O2[j]	3.167 | 2.142	156.43	0.018	0.052	0.013	**15.0**
N5···F4[i]	2.919	-	0.009	0.035	0.008	**9.0**
N3···F1[k]	3.042	-	0.007	0.029	0.006	**7.1**
C8···F4[h]	3.084	-	0.007	0.029	0.006	**6.5**
O3···O7[a]	3.152	-	0.006	0.027	0.006	**6.3**
C2···O5[f]	3.084	-	0.007	0.025	0.005	**6.1**
C3···O3[k]	3.093	-	0.007	0.026	0.005	**5.9**
O7···O1[b]	3.412	-	0.006	0.024	0.005	**5.9**
F4···F2[j]	3.003	-	0.004	0.026	0.005	**5.8**
F4···F1[j]	3.010	-	0.004	0.026	0.005	**5.7**
F2···F3[h]	3.015	-	0.004	0.026	0.005	**5.7**
O2···N1[b]	3.234	-	0.006	0.021	0.005	**5.3**
C8···C16[h]	3.167	-	0.007	0.024	0.005	**5.2**
N7···O4[h]	3.271	-	0.006	0.021	0.005	**5.2**
C4···N2[b]	3.246	-	0.007	0.021	0.004	**5.1**
C8···C12[l]	3.241	-	0.007	0.023	0.004	**5.0**
O6···N4[l]	3.294	-	0.005	0.020	0.004	**4.9**
C12···N6[a]	3.251	-	0.006	0.021	0.004	**4.9**
N3···O6[l]	3.319	-	0.005	0.020	0.004	**4.9**
C16···O5[j]	3.259	-	0.006	0.021	0.004	**4.8**
O7···N7[m]	3.277	-	0.005	0.020	0.004	**4.7**
N5···O6[a]	3.329	-	0.005	0.019	0.004	**4.6**
N1···O1[n]	3.285	-	0.005	0.019	0.004	**4.6**
O4···F3[l]	3.234	-	0.004	0.020	0.004	**4.5**
C14···O1[o]	3.307	-	0.005	0.019	0.004	**4.2**
N8···O4[h]	3.419	-	0.004	0.017	0.004	**4.1**
C11···N8[l]	3.497	-	0.004	0.013	0.003	**2.9**
E_{latt} (kJ/mol)						**108.9**

* The electron density ρ_b, Laplacian of electron density $\nabla^2\rho_b$ and local electronic kinetic energy density G_b at the bond critical point; the energy of the intermolecular noncovalent interaction E_{int}. The level of theory in the DFT computations is B3LYP-D3(BJ)/6-31(F+)G(d,p).

Symmetry codes: [a] -x,-1-y,-z; [b] -x,-y,-1-z; [c] x,y,1+z; [d] x,y,-1+z;[e] 1-x,-1-y,-z; [f] x,1+y,z; [g] -1+x,y,-1+z; [h] -x,-y,-z; [i] 1+x,y,z; [j] -1+x,y,z; [k] 1-x,-y,-z; [l] x,y,z; [m] -1-x,-1-y,-1-z; [n] -x,1-y,-1-z; [o] -1-x,-y,-1-z.

Table S7. Metric and Electron Density Properties in Bond Critical Point of Noncovalent Interactions in 3HNA (refcode HNAPAC01) Obtained from Periodic DFT Calculations Followed by Bader Analysis of Periodic Electron Density *

non-covalent interaction	D···A (Å) | H···A (Å)	∠D–H···A (°)	ρ_b (a.u.)	$\nabla^2\rho_b$ (a.u.)	G_b (a.u.)	E_{int} (kJ/mol)
O11−H11···O2[a]	2.637 | 1.634	176.62	0.051	0.145	0.038	**42.9**
O3−H10···O2[b]	2.618 | 1.735	147.62	0.043	0.130	0.034	**37.9****
C4−H4···C1[c]	3.700 | 2.633	168.29	0.009	0.027	0.006	**6.4**
C9−H9···O3[d]	3.614 | 2.628	150.81	0.007	0.024	0.005	**6.0**
H8···H8[e]	2.304	-	0.006	0.025	0.005	**5.2**
C6−H6···O1[f]	3.272 | 2.746	109.47	0.006	0.023	0.005	**5.2**
C9···O1[g]	3.291	-	0.006	0.019	0.004	**4.5**
C8−H8···O2[h]	3.517 | 2.810	122.84	0.005	0.019	0.004	**4.3**
C2···O3[i]	3.387	-	0.005	0.018	0.004	**4.0**
C5···C1[j]	3.327	-	0.006	0.018	0.004	**4.0**
C9···C3[j]	3.370	-	0.006	0.016	0.003	**3.7**
C6−H6···C8[c]	4.012 | 2.948	166.79	0.005	0.015	0.003	**3.5**
C7···C11[j]	3.463	-	0.004	0.013	0.003	**2.8**
C7−H7···O2[k]	3.859 | 2.994	136.81	0.003	0.012	0.002	**2.6**
C1−H1···C4[l]	4.098 | 3.123	149.94	0.003	0.010	0.002	**2.2**
E_{latt} (kJ/mol)						**97.3**

* The electron density ρ_b, Laplacian of electron density $\nabla^2\rho_b$ and local electronic kinetic energy density G_b at the bond critical point; the energy of the intermolecular noncovalent interaction E_{int}. The level of theory in the DFT computations is B3LYP-D3(BJ)/6-31G(d,p).

** Intramolecular contact. The energy of this interaction does not count in the total E_{latt} value.

Symmetry codes: [a] -x,-1-y,-z; [b] x,y,z; [c] x,-1/2-y,-1/2+z; [d] -1-x,-1/2+y,-1/2-z; [e] -2-x,-1-y,-1-z; [f] -1-x,1/2+y,-1/2-z; [g] -1-x,-1-y,-z; [h] -1+x,y,z; [i] x,-1/2-y,1/2+z; [j] -1-x,-1-y,-1-z; [k] -1+x,-1/2-y,-1/2+z; [l] -1-x,-1/2+y,-1/2-z.

Table S8. Metric and Electron Density Properties in Bond Critical Point of Noncovalent Interactions in 6HNA (refcode JACDAV) Obtained from Periodic DFT Calculations Followed by Bader Analysis of Periodic Electron Density *

non-covalent interaction	D···A (Å) | H···A (Å)	∠D–H···A (°)	ρ_b (a.u.)	$\nabla^2\rho_b$ (a.u.)	G_b (a.u.)	E_{int} (kJ/mol)
O12–H12···O13[a]	2.641 | 1.654	167.93	0.050	0.141	0.037	**41.3**
O14–H14···O13[b]	2.850 | 1.895	164.96	0.026	0.080	0.020	**22.1**
C5–H5···O12[c]	3.514 | 2.521	151.72	0.008	0.027	0.006	**6.8**
H7···H7[d]	2.165	-	0.008	0.030	0.006	**6.5**
C7–H7···O14[d]	3.564 | 2.652	141.54	0.006	0.023	0.005	**5.6**
O14···O13[e]	3.254	-	0.005	0.021	0.004	**5.0**
O14···O12[f]	3.234	-	0.005	0.021	0.004	**5.0**
H1···H4[g]	2.275	-	0.006	0.021	0.004	**4.5**
H1···H4[h]	2.450	-	0.006	0.021	0.004	**4.3**
C3–H3···O14[i]	3.763 | 2.754	154.82	0.004	0.017	0.003	**3.9**
H8···H5[h]	2.513	-	0.005	0.019	0.003	**3.9**
C6···O13[e]	3.349	-	0.005	0.017	0.003	**3.8**
C7···O12[e]	3.392	-	0.005	0.016	0.003	**3.7**
H8···H4[h]	2.454	-	0.005	0.017	0.003	**3.6**
C5···C2[e]	3.559	-	0.005	0.014	0.003	**3.2**
C3–H3···O12[j]	3.710 | 2.916	130.23	0.004	0.015	0.003	**3.2**
C1···C9[e]	3.523	-	0.004	0.013	0.003	**2.9**
H8···H4[g]	2.675	-	0.004	0.014	0.003	**2.9**
C4···C10[e]	3.654	-	0.004	0.011	0.002	**2.6**
C2···C8[e]	3.655	-	0.004	0.011	0.002	**2.5**
E_{latt} (kJ/mol)						**137.4**

* The electron density ρ_b, Laplacian of electron density $\nabla^2\rho_b$ and local electronic kinetic energy density G_b at the bond critical point; the energy of the intermolecular noncovalent interaction E_{int}. The level of theory in the DFT computations is B3LYP-D3(BJ)/6-31G(d,p).

Symmetry codes: [a] -1-x,-y,-1-z; [b] -x,-1/2+y,-1/2-z; [c] 1+x,-1/2-y,1/2+z; [d] -1-x,-1-y,-1-z; [e] x,-1/2-y,1/2+z; [f] -1-x,-1/2+y,-1/2-z; [g] -1+x,-1/2-y,-1/2+z; [h] -1+x,y,z; [i] -x,1/2+y,-1/2-z; [j] 1+x,y,z.

Table S9. Total Electronic Energies of Crystals (E_{total}), Zero-Point Energies (ZPE) and Thermal Corrections (E_{thetm}), Pressure-Volume Term (pV), Entropy Corrections (TS), Total Free Gibbs Energies of Crystals (G_{total}), Cocrystal Formation Energies (E_{form}) and Cocrystal Formation Gibbs Energies (G_{form}) Obtained from Periodic DFT-D3 Calculations

Crystal	**5FU**	**3HNA**	**6HNA**
Z	8	4	4
E_{total}, a.u./cell	-4111.0300960778	-2597.8047106328	-2597.8171292864
ZPE, a.u./cell	0.6506264996	0.6779523388	0.6773718352
E_{therm}, a.u./cell	0.0621567288	0.0444294205	0.0445606489
pV, a.u./cell	0.0000224342	0.0000200140	0.0000195203
TS, a.u./cell	0.1229399300	0.0862086865	0.0858781941
G_{total}, a.u./cell	-4110.4402303451	-2597.1685175461	-2597.1810554761
Crystal	**5FU-3HNA** (conformation 1)	**5FU-3HNA** (conformation 2)	**5FU-6HNA**
Z	4	4	4
E_{total}, a.u./cell	-6708.8362882610	-6708.8364863387	-4653.3368656022
ZPE, a.u./cell	1.3281201675	1.3281035777	1.0021664922
E_{therm}, a.u./cell	0.1092585034	0.1094005632	0.0767691508
pV, a.u./cell	0.0000420309	0.0000420309	0.0000312033
TS, a.u./cell	0.2197707359	0.2202886324	0.1513643468
G_{total}, a.u./cell	-6707.6186382951	-6707.6192287992	-4652.4092631026
E_{form}, kJ/mol	-1.3		-3.4
G_{form}, kJ/mol	-6.7		-5.3

Table S10. Cumulative Amount Per Unit Area Permeated (Q_n) in 8 h, Steady Penetration Rate (J_s) and Their Corresponding Ratio of Cocrystals to Parent 5FU

sample	Q_n (μg/cm^2)	ratio of Q_n	J_s (μg/cm^2/h)	ratio of J_s
5FU*	14.57(1.38)	1	1.84(0.02)	1
5FU-3HBA*	20.70(0.32)	1.42	2.55(0.03)	1.39
5FU-4ABA*	24.00(1.22)	1.65	3.02(0.03)	1.64
5FU-CA*	27.28(0.73)	1.87	3.37(0.07)	1.83
5FU**	9.72(0.36)	1	1.24(0.01)	1
5FU-3HBA**	13.61(0.55)	1.40	1.72(0.02)	1.39
5FU-4HBA I**	13.84(0.13)	1.42	1.72(0.02)	1.39
5FU-4HBA II**	15.92(0.82)	1.64	1.98(0.01)	1.60
5FU-SA**	11.11(0.40)	1.14	1.38(0.02)	1.11
5FU-3HNA**	11.43(0.21)	1.18	1.35(0.03)	1.08
5FU-6HNA**	16.90(0.56)	1.74	1.99(0.06)	1.60

* The receptor chamber was filled with 8 mL of degassed pH 7.4 phosphate buffer

** The receptor chamber was filled with 17 mL of degassed pH 7.4 phosphate buffer

Table S11. Solubility Value (mg/mL) of 5FU cocrystals at 37 ºC

sample	Solubility (mg/mL)
5FU	19.20(12)*
5FU/3HBA	21.13(36)*
5FU/4ABA	18.99(28)*
5FU/CA	18.07(12)*
5FU	21.19(53)**
5FU-3HBA	22.40(62)**
5FU-SA	17.88(23)**
5FU-4HBA I	21.98(37)**
5FU-4HBA II	24.41(50)**
5FU-6HNA	7.91(12)**
5FU-3HNA	23.37(14)**

* The solubility value was tested in pH 7.4 phosphate buffer

** The solubility value was tested in pH 6.8 phosphate buffer

(a)

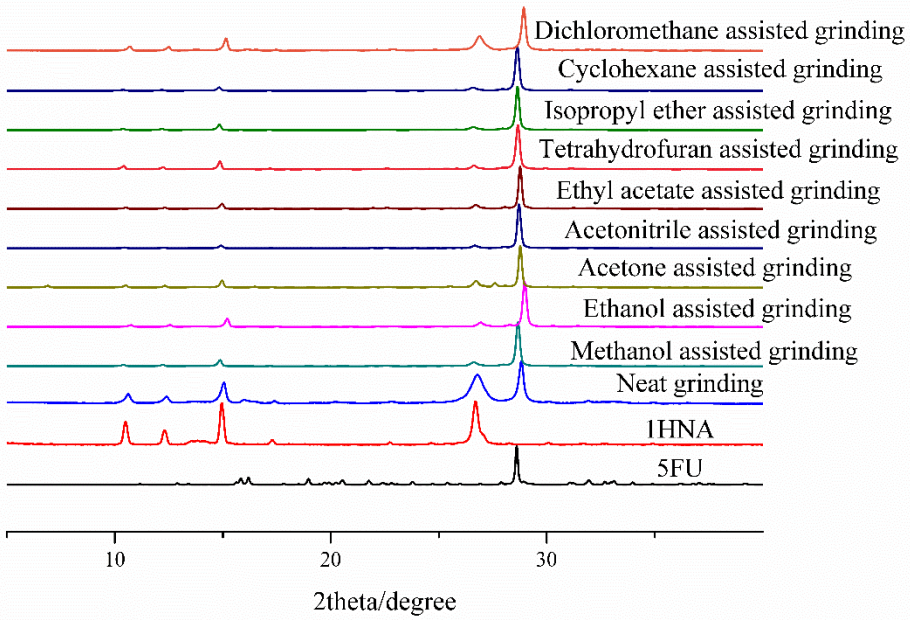
Dichloromethane assisted grinding
Cyclohexane assisted grinding
Isopropyl ether assisted grinding
Tetrahydrofuran assisted grinding
Ethyl acetate assisted grinding
Acetonitrile assisted grinding
Acetone assisted grinding
Ethanol assisted grinding
Methanol assisted grinding
Neat grinding
1HNA
5FU
10
20
30
2theta/degree

(b)

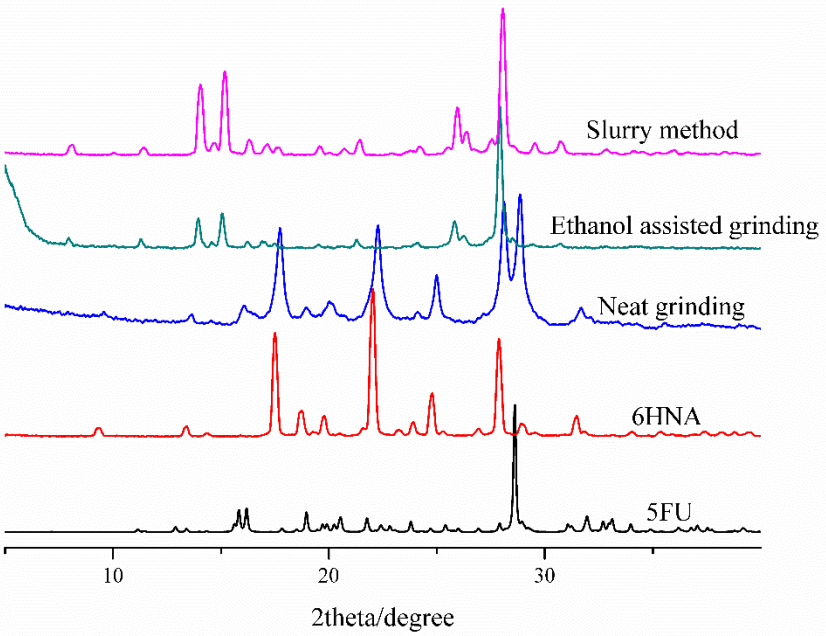
Slurry method
Ethanol assisted grinding
Neat grinding
6HNA
5FU
10
20
30
2theta/degree

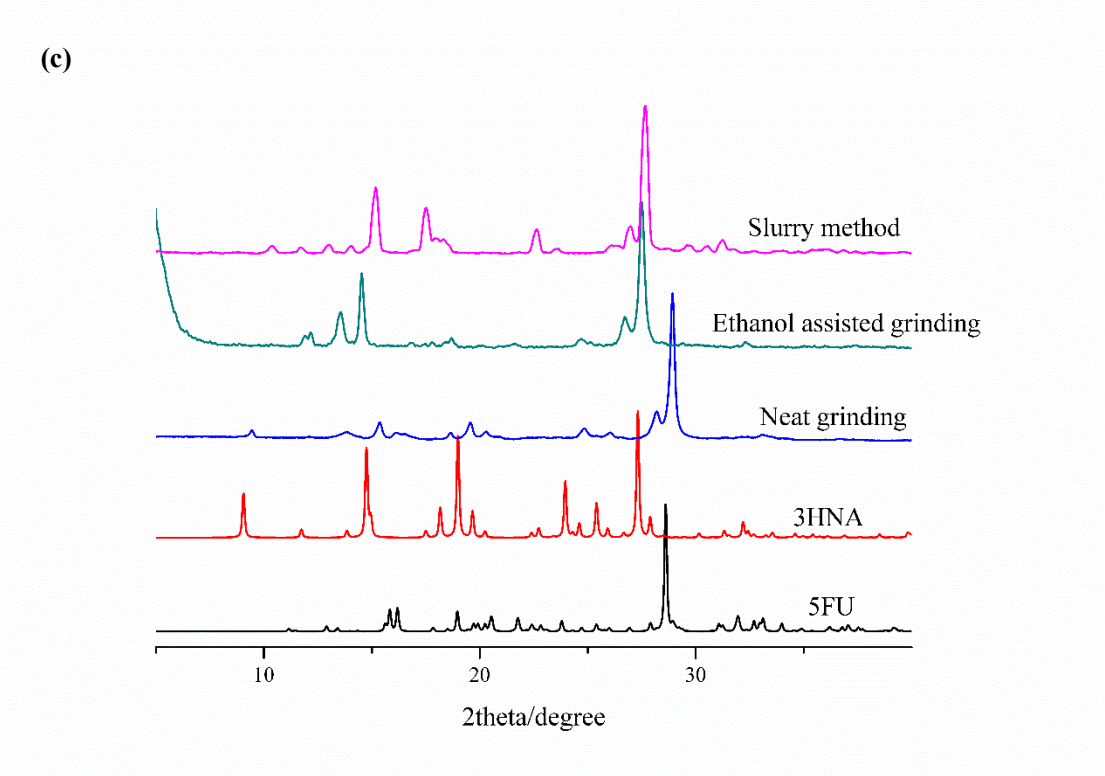

Figure S1. PXRD patterns of the grinding and slurry outcome of (a) 5FU and 1HNA, (b) 5FU and 6HNA and (c) 5FU and 3HNA.

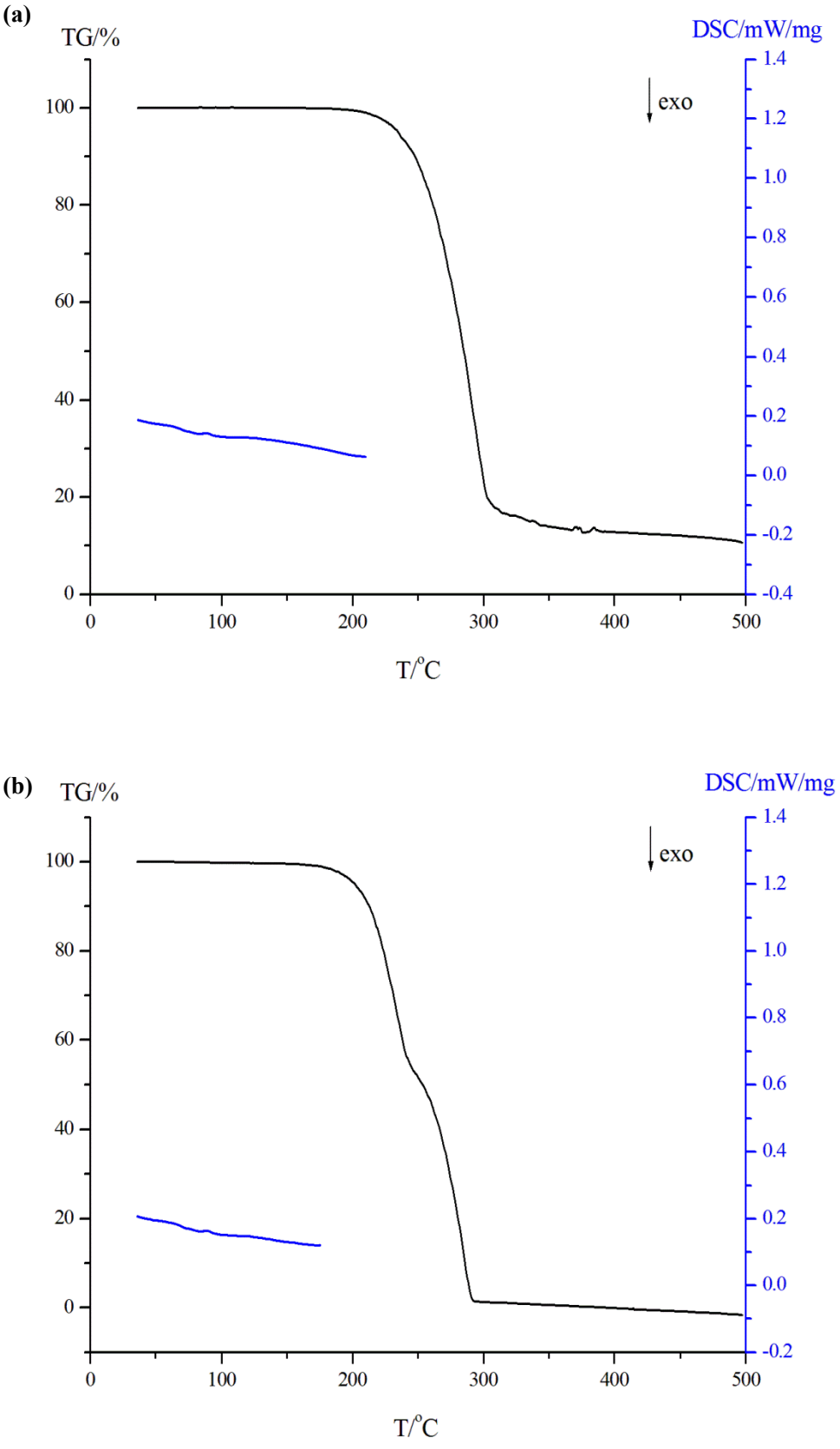

Figure S2. DSC-TG curves for (a) **5FU-6HNA** and (b) **5FU-3HNA**.

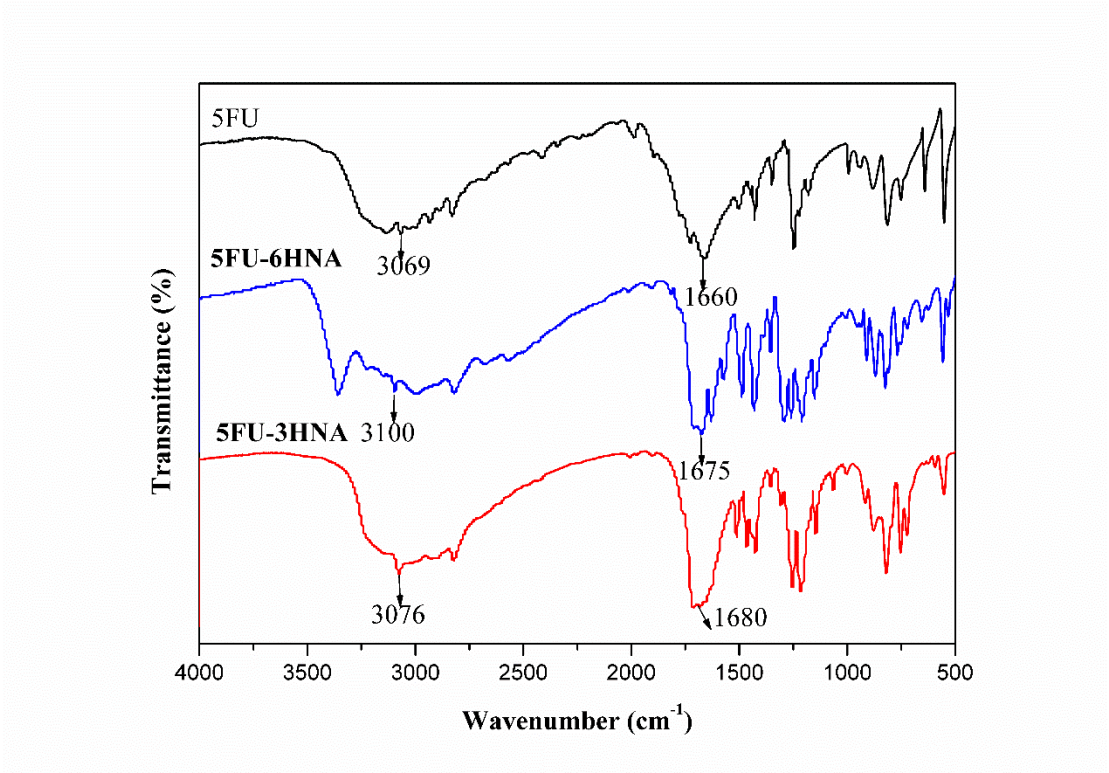

Figure S3. IR spectrogram of 5FU and its cocrystals.

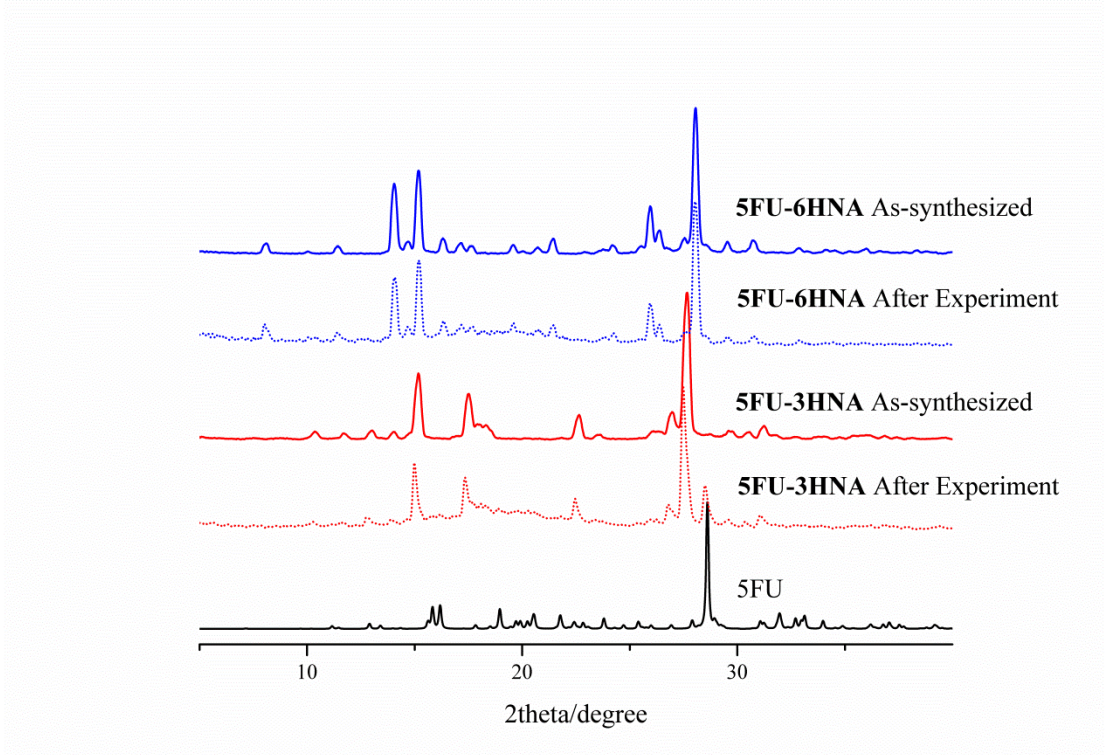

Figure S4. PXRD patterns of cocrystals after permeation experiment.

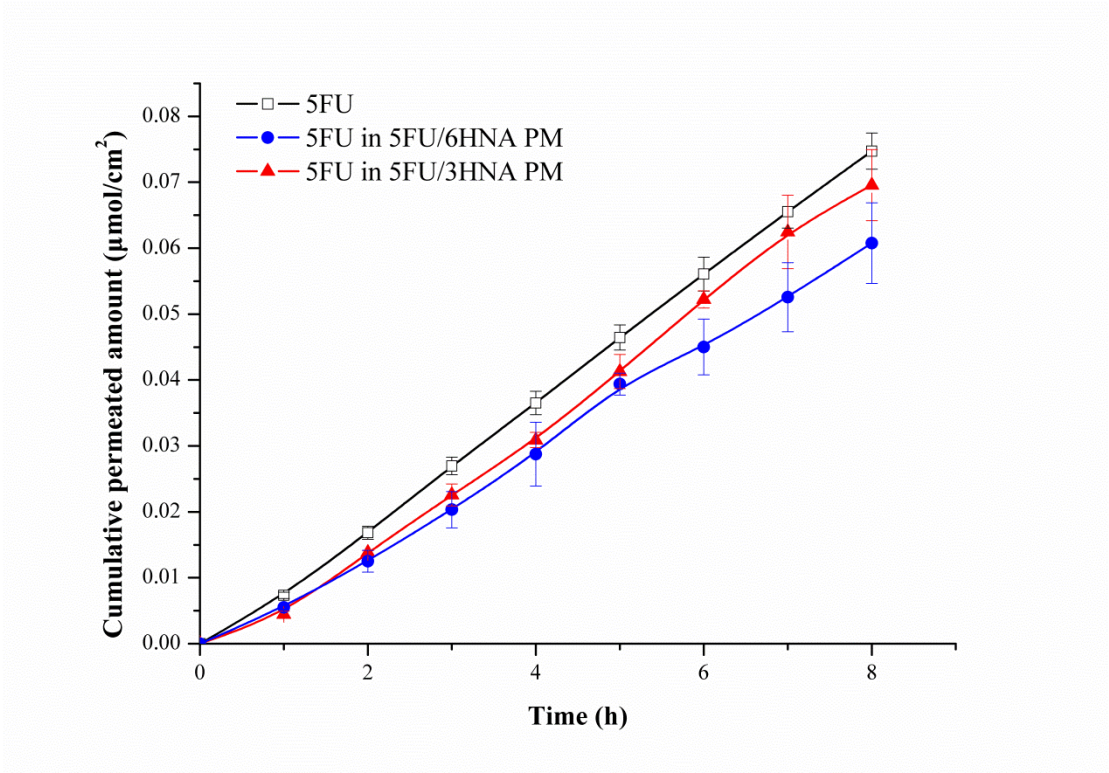

Figure S5. Cumulative permeated amount per unit area of 5FU and the physical mixtures.

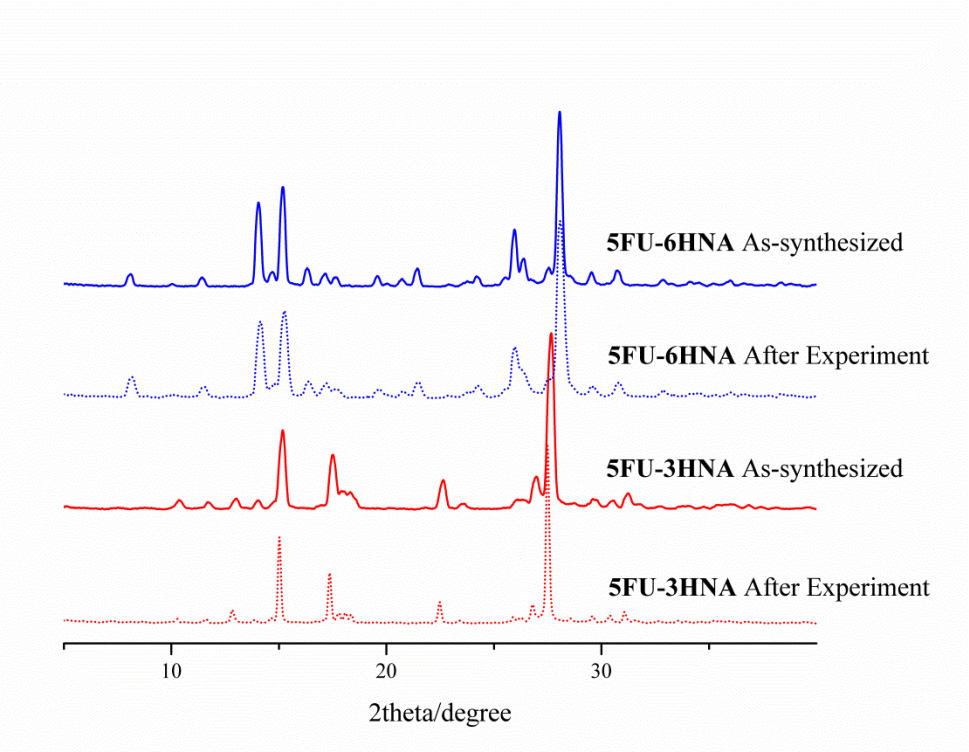

Figure S6. PXRD patterns of cocrystals after solubility test in pH 6.8 phosphate buffer.

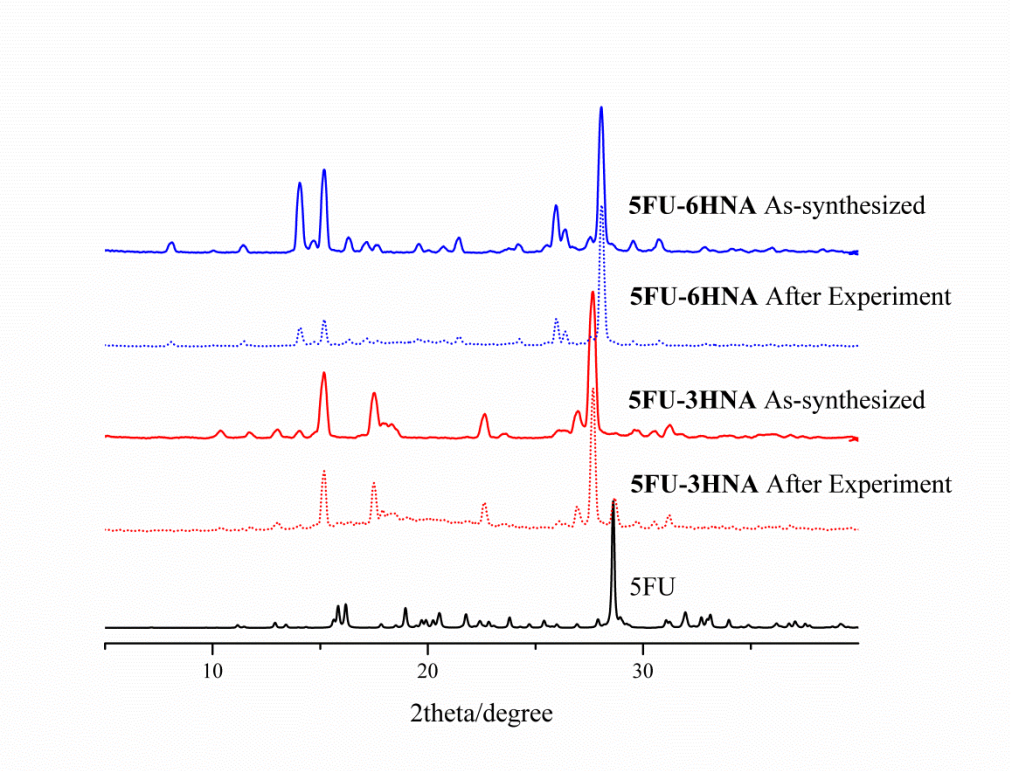

Figure S7. PXRD patterns of cocrystals after dissolution experiment in IPM.